# Chapter 5

# A parameter uniform numerical method for class of singularly perturbed parabolic partial differential equations with multiple boundary turning point

## 5.1 Introduction

A numerical scheme for singularly perturbed parabolic boundary value problems including multiple boundary turning points at left endpoint of the spatial direction is developed. The highest order derivative of these problems is multiplied by $\varepsilon(0<\varepsilon\ll 1)$ and for small $\varepsilon$ close to zero, the solution of these problems exhibits a boundary layer of parabolic type near the left lateral surface of the domain of consideration. Thus, the large oscillations appear when the problem is solved by classical/standard numerical methods and the expected accuracy cannot be achieved *i.e.,* the accuracy of the methods depend continuously on $\varepsilon$. In this chapter, an attempt has been made to resolve this difficulty by suggesting the Crank-Nicolson scheme on a uniform mesh in the temporal direction and an upwind scheme on a piecewise-uniform mesh (Shishkin-type mesh) in the spatial direction. Sharper bounds (which are used in the parameter uniform convergence analysis) on the smooth and singular components and their derivatives are established. Through a rigorous analysis theoretical results are proved which show that the method converges irrespective of the size of $\varepsilon$ and is of $\mathscr{O}((\Delta t)^2+N^{-1}\ln N)$. Two test examples are encountered to verify the computational results with the theoretical results.

Let $\Omega=(0,1), \Lambda=(0,T], \mathscr{D}=\Omega\times\Lambda$, with boundary $\Gamma=\Gamma_l\cup\Gamma_b\cup\Gamma_r$, where $\Gamma_l=\{(0,t)\,|\,0\le t\le T\}, \Gamma_b=\{(x,0)\,|\,0\le x\le 1\}$ and $\Gamma_r=\{(1,t)\,|\,0\le t\le T\}$ are the

left, bottom and the right boundaries of $\mathscr{D}$. In this chapter, we consider the following problem

$$L\psi(x,t) \equiv -\psi_t + \varepsilon\psi_{xx} + a(x,t)\psi_x - b(x,t)\psi = f(x,t), \quad (x,t) \in \mathscr{D}, \tag{5.1a}$$

$$\psi(x,0) = \psi_b(x), \quad x \in \overline{\Omega}, \tag{5.1b}$$

$$\psi(0,t) = \psi_l(t) \text{ on } \Gamma_l, \tag{5.1c}$$

$$\psi(1,t) = \psi_r(t) \text{ on } \Gamma_r, \tag{5.1d}$$

where $0 < \varepsilon \ll 1$ is diffusion parameter. The following assumptions are made which ensure that the problem (5.1) has a unique solution.

- The functions $a(x,t),\ b(x,t),\ f(x,t)$ in $\overline{\mathscr{D}}$ and $\psi_l(t),\ \psi_r(t),\ \psi_b(x)$ on $\Gamma$ are smooth enough and bounded.
- $a(x,t) = a^*(x,t)x^p,\ p \geq 1$ where $a^*(x,t)$ is smooth and satisfies $a^*(x,t) \leq \alpha < 0,\ (x,t) \in \overline{\mathscr{D}}$.
- $b(x,t) \geq \beta > 0,\ (x,t) \in \overline{\mathscr{D}}$.
- The initial function satisfies the compatibility conditions.

The layer behavior of the SPBVPs is characterized in different categories by the sign of $a(x,t)$. If $a(x,t)$ is positive throughout $\overline{\mathscr{D}}$, a regular/exponential boundary layer appears near the left lateral surface of the domain while if $a(x,t)$ is negative throughout $\overline{\mathscr{D}}$, a regular/exponential boundary layer appear near the right lateral surface of the domain. On the other hand for $a(x,t)$ identically zero throughout $\overline{\mathscr{D}}$, there are parabolic boundary layers at both ends. Although in our problem, the form of $a(x,t)$ is different from the above cases but a parabolic boundary layer appears in the solution near the left lateral surface $\Gamma_l$. The boundary layer behavior of the SPBVPs leads to the failure of the classical/standard numerical methods unless an unacceptably large number of mesh elements is used, which is practically too tedious. Therefore, we require a method, probably on a non-uniform mesh, which is convergent irrespective of the size of $\varepsilon$ in some discrete norm.

The summary of the chapter is as follows. Some *a priori* estimates are established in Section 5.2. In particular, the bounds on the derivatives of the solution and the minimum principle are established. Furthermore, the sharper bounds on the smooth and singular components and their derivatives are also given. The temporal semi-discretization and the local, as well as global error estimates in the temporal direction,

are obtained in Section 5.3. Furthermore, the discretization of the system of ODEs obtained in the temporal semi-discretization by using a finite difference scheme on a Shishkin-type mesh is also constructed in this section. The main result of the convergence is proved in Section 5.4 followed by some numerical experiments and the discussion on the results in Section 5.5. Finally, in the end, some concluding remarks and the future scope is included in the last Section 5.6.

## 5.2 Continuous Problem

In this section, we establish some *a priori* results like minimum principle, stability estimate, bounds estimates on the derivatives, etc. The proof of the following minimum principle is straightforward and can be proved by following the approach given in [129].

**Lemma 5.2.1.** *Let $\Phi \in C^{2,1}(\overline{\mathscr{D}})$ be non-negative on $\Gamma$ and $L\Phi$ is non-positive in the interior of $\mathscr{D}$. Then, $\Phi$ is non-negative throughout $\overline{\mathscr{D}}$.*

The stability lemma given below can also be proved in a classical way.

**Lemma 5.2.2.** *The $\varepsilon$-uniform bound on the solution $\psi(x,t)$ of (5.1) is given by*

$$\|\psi\|_{\overline{\mathscr{D}}} \leq \|\psi\|_{\Gamma} + \frac{\|f\|_{\overline{\mathscr{D}}}}{\beta}.$$

*Proof.* For the proof, one can see Chapter 4. □

The proof of the next theorem is based on the following lemmas and the assumption that the function $a(x,t)$ in (5.1) is independent of $t$, *i.e.,* $a = a(x)$.

**Lemma 5.2.3.** *(Bobisud [130]). The solution $\psi(x,t)$ of (5.1) can be written as $\psi(x,t) = v_1(x,t) + \varepsilon v_2(x,t) + p(x,t)$, where $v_1$ and $v_2$ satisfy parabolic equations similar to (5.1) with zero initial-boundary conditions and $p$ is independent of $\varepsilon$.*

In the following lemma, we may assume without loss of generality that the initial-boundary conditions are identically zero.

**Lemma 5.2.4.** *If $a(x,t) = a(x)$, then the solution $\psi(x,t)$ of (5.1) satisfies*

$$\left\| \frac{\partial^j \psi}{\partial t^j} \right\|_{\overline{\mathscr{D}}} \leq C, \ j = 1,2.$$

*Proof.* On the left ($x=0$) and right ($x=1$) sides of $\overline{\mathscr{D}}$, we have $\psi \equiv 0$ and thus $\psi_t \equiv 0$. On the bottom side ($t=0$), we have $y \equiv 0$ and so $\psi_x \equiv \psi_{xx} \equiv 0$ which from (5.1) yields

$$\psi_t(x,0) = -f(x,0),\ 0 \le x \le 1.$$

Thus $\psi_t$ is bounded on $\Gamma$. Now for $(x,t) \in \mathscr{D}$, we have

$$\begin{aligned} L\psi_t &= \varepsilon \psi_{txx} + a\psi_{tx} - b\psi_t - \psi_{tt} \\ &= (\varepsilon \psi_{xx} + a\psi_x - b\psi - \psi_t)_t + b_t \psi \\ &= f_t + b_t \psi, \end{aligned}$$

so $|L\psi_t| \le C$. Hence, by using minimum principle we have $|\psi_t| \le C$, $\forall\,(x,t) \in \overline{\mathscr{D}}$. The second derivative bound of $\psi$ with respect to $t$ can be estimated in the same way. □

**Lemma 5.2.5.** *The solution $\psi(x,t)$ of the problem (5.1) and its derivatives with respect to x satisfy the following bounds*

$$\left\| \frac{\partial^i \psi}{\partial x^i} \right\|_{\overline{\mathscr{D}}} \le C\left(1 + \varepsilon^{-i/2} e^{-x\sqrt{\beta/\varepsilon}}\right), \quad 1 \le i \le 4.$$

*Proof.* Fix a fixed $t \in [0,T]$, the result can be obtained by applying the argument of Kellog and Tsan [116] (Lemmas 2.2 and 2.3) on the line segment $\{(x,t) : 0 \le x \le 1\}$. □

The following theorem can be proved by combining the results of Lemmas 5.2.4 and 5.2.5.

**Theorem 5.2.1.** *The mixed derivatives of the solution $\psi(x,t)$ of (5.1) satisfy the following bounds*

$$\left\| \frac{\partial^{i+j} \psi}{\partial x^i \partial t^j} \right\|_{\overline{\mathscr{D}}} \le C\left(1 + \varepsilon^{-i/2} e^{-x\sqrt{\beta/\varepsilon}}\right), \quad 0 \le i + 3j \le 4.$$

## 5.3 Description of the Numerical Scheme

To discretize the problem in the temporal direction, we divide the interval $[0,T]$ in $M$ equally distributed parts each of width $\Delta t = T/M$. Thus the mesh in the temporal

direction is

$$\Lambda^M = \{t_j = j\Delta t : \ j = 0,1,\ldots,M\}.$$

Then on $\Omega \times \Lambda^M$, problem (5.1) is discretized as follows

$$\begin{aligned}
&-D_t^- u^{j+1}(x) + \varepsilon (u_{xx})^{j+1/2} + a^{j+1/2}(x)(u_x)^{j+1/2} - b^{j+1/2}(x)u^{j+1/2} = f^{j+1/2}(x),\\
&\qquad x \in \Omega,\ 0 \le j \le M-1,\\
&u^{j+1}(0) = \psi_l(t_{j+1}),\ u^{j+1}(1) = \psi_r(t_{j+1}), \quad 0 \le j \le M-1,\\
&u^0(x) = \psi_b(x), \quad x \in \Omega,
\end{aligned}$$

where $u^{j+1}(x)$ is the approximation of $\psi(x,t_{j+1})$, $D_t^- z^j(x) = \frac{z^j(x)-z^{j-1}(x)}{\Delta t}$ and $z^{j+1/2}(x) = \frac{z^{j+1}(x)+z^j(x)}{2}$, etc. Rewrite the above equation as

$$\begin{cases}
\hat{L}u^{j+1}(x) = g(x,t_{j+1}), & x \in \Omega,\ 0 \le j \le M-1,\\
u^{j+1}(0) = \psi_l(t_{j+1}),\ u^{j+1}(1) = \psi_r(t_{j+1}), & 0 \le j \le M-1,\\
u^0(x) = \psi_b(x), \quad x \in \Omega,
\end{cases} \tag{5.2}$$

where

$$\begin{aligned}
\hat{L} &\equiv \frac{\varepsilon}{2}\frac{d^2}{dx^2} + \frac{a^{j+1/2}(x)}{2}\frac{d}{dx} - \frac{c^{j+1/2}(x)}{2}I,\\
g(x,t_{j+1}) &= f^{j+1/2}(x) - \frac{\varepsilon}{2}(u_{xx})^j(x) - \frac{a^{j+1/2}(x)}{2}(u_x)^j(x) + \frac{d^{j+1/2}(x)}{2}u^j(x),\\
d^{j+1/2}(x) &= b^{j+1/2}(x) - \frac{2}{\Delta t}, \quad c^{j+1/2}(x) = b^{j+1/2}(x) + \frac{2}{\Delta t}.
\end{aligned}$$

**Lemma 5.3.1.** *If $\Phi^{j+1}(0)$ and $\Phi^{j+1}(1)$ are non-negative and $\hat{L}\Phi^{j+1} \le 0$ on $\Omega$, then $\Phi^{j+1}(x) \ge 0$ on $\overline{\Omega}$.*

*Proof.* Suppose there exists $s \in \Omega$, such that $\Phi^{j+1}(s) = \min_{x\in\Omega}\Phi^{j+1}(x) < 0$. It follows that $(\Phi^{j+1})'(s) = 0$ and $(\Phi^{j+1})''(s) \ge 0$. Then, we have

$$\hat{L}\Phi^{j+1}(s) = \frac{\varepsilon}{2}(\Phi^{j+1})''(s) + \frac{a^{j+1/2}(s)}{2}(\Phi^{j+1})'(s) - \frac{c^{j+1/2}(s)}{2}\Phi^{j+1}(s) > 0,$$

as $c^{j+1/2}(s) = b^{j+1/2}(s) + \frac{2}{\Delta t} \geq \beta + \frac{2}{\Delta t} > 0$. Thus, the proof is completed by contradiction. □

The local truncation error $e_{j+1}$ of the temporal semi-discretization defined as $e_{j+1} = u^{j+1}(x) - \widetilde{u}(x)$, where $\widetilde{u}(x)$ is the computed solution of (5.2) satisfies the following estimate

**Lemma 5.3.2.** *The local truncation error estimate is given by*

$$\|e_{j+1}\| \leq C(\Delta t)^3, \ j = 0, 1, \ldots, M-1.$$

*Proof.* Using Taylor theorem, we have

$$\psi(x,t_{j+1}) = \psi(x,t_{j+1/2}) + \frac{\Delta t}{2}\psi_t(x,t_{j+1/2}) + \frac{(\Delta t)^2}{8}\psi_{tt}(x,t_{j+1/2}) + O((\Delta t)^3),$$
$$\psi(x,t_j) = \psi(x,t_{j+1/2}) - \frac{\Delta t}{2}\psi_t(x,t_{j+1/2}) + \frac{(\Delta t)^2}{8}\psi_{tt}(x,t_{j+1/2}) + O((\Delta t)^3).$$

On subtracting, it gives

$$\begin{aligned}\frac{\psi(x,t_{j+1}) - \psi(x,t_j)}{\Delta t} &= \psi_t\left(x, t_j + \frac{\Delta t}{2}\right) + O((\Delta t)^2) \\ &= \varepsilon\psi_{xx}(x,t_{j+1/2}) + a(x,t_{j+1/2})\psi_x(x,t_{j+1/2}) \\ &\quad - b(x,t_{j+1/2})\psi(x,t_{j+1/2}) - f(x,t_{j+1/2}) + O((\Delta t)^2),\end{aligned}$$

where $a(x,t_{j+1/2}) = \frac{a(x,t_{j+1})+a(x,t_j)}{2}$, etc. So, we can see that the local error is the solution of

$$\hat{L}e_{j+1} = O((\Delta t)^3),$$

$$e_{j+1}(0) = e_{j+1}(1) = 0.$$

Hence, by using the minimum principle we get the required result. □

Furthermore, the following estimate for the global error $E_j$ of the time semi-discretization can be proved by contributing to the local truncation errors and an application of Lemma 5.3.2.

**Theorem 5.3.1.** *The global error estimate satisfies*

$$\|E_j\| \leq C(\Delta t)^2, \quad 0 \leq j \leq M.$$

The following estimates on $u^{j+1}(x)$ and its derivatives can be proved by following the technique given in [116].

**Theorem 5.3.2.**

$$\left|\frac{d^k}{dx^k}u^{j+1}(x)\right| \leq C(1+\varepsilon^{-k/2}\exp(-x\sqrt{\beta/\varepsilon})), \quad k=0,1,2,3.$$

We further decompose the solution $u^{j+1}(x)$ as

$$u^{j+1}(x) = \psi^r(x,t_{j+1}) + \psi^s(x,t_{j+1}), \quad x \in \overline{\Omega},$$

where the regular and singular components $\psi^r(x,t_{j+1})$ and $\psi^s(x,t_{j+1})$ satisfy the following estimates.

**Theorem 5.3.3.**

$$\left|\frac{d^k\psi^r(x,t_{j+1})}{dx^k}\right| \leq C(1+\varepsilon^{(1-k)/2}),\ k=0,1,2,$$

$$\left|\frac{d^k\psi^s(x,t_{j+1})}{dx^k}\right| \leq C\varepsilon^{-k/2}\exp(-x\sqrt{\beta/\varepsilon}),\ k=0,1,2,3.$$

The appearance of the boundary layer suggests us to increase the density of the points in the neighborhood of the layer region. This type of mesh can be constructed by taking $\overline{\Omega} = \Omega_1 \cup \Omega_2$, where $\Omega_1 = [0,\tau],\ \Omega_2 = (\tau,1]$, and the transition parameter $\tau$ is given by

$$\tau = \min\{1/2, \tau^*\sqrt{\varepsilon}\,\ln N\}.$$

Here $N \geq 2$ is the mesh intervals used and $\tau^*$ is a constant that depends on $b(x,t)$ and should be chosen as $\tau^* \geq \frac{1}{\sqrt{\beta}}$. Clearly the mesh $\Omega^N = \{x_i\}_{i=0}^N$ generated in this way is dense in the layer region and is given by

$$x_i = \begin{cases} \frac{2\tau}{N}i, & i=0,1,\ldots,N/2, \\ \tau + \frac{2(1-\tau)}{N}\left(i-\frac{N}{2}\right), & i=N/2+1,\ldots,N, \end{cases}$$

and the mesh spacing is given by

$$h_i = x_i - x_{i-1} = \begin{cases} \frac{2\tau}{N}, & i=1,2,\ldots,N/2, \\ \frac{2(1-\tau)}{N}, & i=N/2+1,\ldots,N. \end{cases}$$

Thus $\mathscr{D}^{N,M} = \Omega^N \times \Lambda^M$ is our fully discretized mesh and $\Gamma^{N,M} = \overline{\mathscr{D}}^{N,M} \cap \Gamma$ is the boundary of the mesh. Introducing the operators

$$D_x^- \mu_i^j = \frac{\mu_i^j - \mu_{i-1}^j}{h_i},\ D_x^+ \mu_i^j = \frac{\mu_{i+1}^j - \mu_i^j}{h_{i+1}},\ \delta_x^2 \mu_i^j = \frac{(D_x^+ - D_x^-)\mu_i^j}{{}_i},$$

where ${}_i = \frac{h_i + h_{i+1}}{2}$ and the notation $\mu_{i-\frac{1}{2}}^j = \frac{\mu_{i-1}^j + \mu_i^j}{2}$, the full discretization of (5.2) on $\mathscr{D}^{N,M}$ is given by

$$\begin{cases} \mathscr{L}^N \widetilde{\psi}(x_i) = \widetilde{g}(x_{i-\frac{1}{2}}), \quad x_i \in \Omega^N, \\ \widetilde{\psi}(x_0) = \psi_l(t_{j+1}), \quad \widetilde{\psi}(x_N) = \psi_r(t_{j+1}),\ 0 \le j \le M-1, \end{cases} \tag{5.3}$$

where $\widetilde{\psi}(x_i) \approx u^{j+1}(x_i)$ and

$$\widetilde{g}(x_{i-\frac{1}{2}}) = f^{j+1/2}(x_{i-\frac{1}{2}}) - \frac{\varepsilon}{2}\delta_x^2 u^j(x_i) - \frac{a^{j+1/2}(x_{i-\frac{1}{2}})}{2} D^- u^j(x_i) + \frac{d^{j+1/2}(x_{i-\frac{1}{2}})}{2} u^j(x_i).$$

The midpoint upwind operator $\mathscr{L}^N$ is given by

$$\mathscr{L}^N \widetilde{\psi} :\equiv \frac{\varepsilon}{2}\delta_x^2 \widetilde{\psi} + \frac{a^{j+1/2}(x_{i-\frac{1}{2}})}{2} D^- \widetilde{\psi} - \frac{c^{j+1/2}(x_{i-\frac{1}{2}})}{2} \widetilde{\psi}.$$

## 5.4 Parameter Uniform Convergence Analysis

The main theorem on the convergence is proved in this section. First, we prove the lemmas which will be used in the proof of the main result.

**Lemma 5.4.1.** *Assume that* $\widetilde{\Phi}(x_0) \ge 0, \widetilde{\Phi}(x_N) \ge 0$ *and* $\mathscr{L}^N \widetilde{\Phi}(x_i) \le 0$ *for all* $x_i \in \Omega^N$ *then* $\widetilde{\Phi}(x_i) \ge 0$ *for all* $x_i \in \Omega^N$.

*Proof.* Suppose $\widetilde{\Phi}(\xi_i) = \min_{x_i \in \Omega^N} \widetilde{\Phi}(\xi_i) < 0$ for some $\xi_i \in \Omega^N$. Then, we have

$$\begin{aligned}
\mathscr{L}^N \widetilde{\Phi}(\xi_i) &= \frac{\varepsilon}{2} \delta_x^2 \widetilde{\Phi}(\xi_i) + \frac{a^{j+1/2}(\xi_{i-\frac{1}{2}})}{2} D^- \widetilde{\Phi}(\xi_i) - \frac{c^{j+1/2}(\xi_{i-\frac{1}{2}})}{2} \widetilde{\Phi}(\xi_i) \\
&= \frac{\varepsilon}{2_i} \left( \frac{\widetilde{\Phi}(\xi_{i+1}) - \widetilde{\Phi}(\xi_i)}{h_{i+1}} - \frac{\widetilde{\Phi}(\xi_i) - \widetilde{\Phi}(\xi_{i-1})}{h_i} \right) \\
&\quad + \frac{a^{j+1/2}(\xi_{i-\frac{1}{2}})}{2} \left( \frac{\widetilde{\Phi}(\xi_i) - \widetilde{\Phi}(\xi_{i-1})}{h_i} \right) - \frac{c^{j+1/2}(\xi_{i-\frac{1}{2}})}{2} \widetilde{\Phi}(\xi_i) > 0.
\end{aligned}$$

Hence the proof is completed by contradiction. □

**Lemma 5.4.2.** *Let the function $\widetilde{\Phi}(x_i)$ vanishes at both end points of $\Omega^N$. Then*

$$|\widetilde{\Phi}(x_i)| \leq \max_{x_i \in \Omega^N} |\mathscr{L}^N \widetilde{\Phi}(x_i)|, \; x_i \in \Omega^N.$$

*Proof.* For the barrier functions $\Psi^{\pm}(x_i) = \max_{x_i \in \Omega^N} |\mathscr{L}^N \widetilde{\Phi}(x_i)| \pm \widetilde{\Phi}(x_i)$, we have

$$\begin{aligned}
\Psi^{\pm}(x_0) &= \max_{x_i \in \Omega^N} |\mathscr{L}^N \widetilde{\Phi}(x_i)| \pm \widetilde{\Phi}(x_0) = \max_{x_i \in \Omega^N} |\mathscr{L}^N \widetilde{\Phi}(x_i)| \geq 0, \\
\Psi^{\pm}(x_N) &= \max_{x_i \in \Omega^N} |\mathscr{L}^N \widetilde{\Phi}(x_i)| \pm \widetilde{\Phi}(x_N) = \max_{x_i \in \Omega^N} |\mathscr{L}^N \widetilde{\Phi}(x_i)| \geq 0.
\end{aligned}$$

Also,

$$\begin{aligned}
\mathscr{L}^N \Psi^{\pm}(x_i) &= \mathscr{L}^N \left[ \max_{x_i \in \Omega^N} |\mathscr{L}^N \widetilde{\Phi}(x_i)| \pm \widetilde{\Phi}(x_i) \right] \\
&= -\frac{c^{j+1/2}(x_{i-1/2})}{2} \max_{x_i \in \Omega^N} |\mathscr{L}^N \widetilde{\Phi}(x_i)| \pm \mathscr{L}^N \widetilde{\Phi}(x_i) \\
&= -\frac{1}{2} \left( b^{j+1/2}(x_{i-1/2}) + \frac{2}{\Delta t} \right) \max_{x_i \in \Omega^N} |\mathscr{L}^N \widetilde{\Phi}(x_i)| \pm \mathscr{L}^N \widetilde{\Phi}(x_i) \\
&\leq \left( \frac{-\beta}{2} - \frac{1}{\Delta t} \right) \max_{x_i \in \Omega^N} |\mathscr{L}^N \widetilde{\Phi}(x_i)| \pm \mathscr{L}^N \widetilde{\Phi}(x_i) \\
&\leq -|\mathscr{L}^N \widetilde{\Phi}(x_i)| \pm \mathscr{L}^N \widetilde{\Phi}(x_i) \\
&\leq 0.
\end{aligned}$$

The proof is completed by applying Lemma 5.4.1. □

**Theorem 5.4.1.** *The error estimate at $(j+1)$-th time level is given by*

$$|\psi(x_i,t_{j+1}) - \widetilde{\psi}_i| \leq CN^{-1}\ln N, \quad i = 0,1,\ldots,N.$$

*Proof.* We'll prove the result by decomposing the solution $\widetilde{\psi}_i$ as

$$\widetilde{\psi}_i = \widetilde{\psi}_i^r + \widetilde{\psi}_i^s,$$

where $\widetilde{\psi}_i^r$ and $\widetilde{\psi}_i^s$ satisfy the following inhomogeneous and homogeneous problems respectively

$$\begin{aligned}
&\mathscr{L}^N\widetilde{\psi}_i^r = \widetilde{g}(x_{i-1/2}) \text{ in } \mathscr{D}^{N,M}, \quad \widetilde{\psi}_i^r = \psi^r(x_i,t_{j+1}) \text{ on } \Gamma^{N,M},\\
&\mathscr{L}^N\widetilde{\psi}_i^s = 0 \text{ in } \mathscr{D}^{N,M}, \quad \widetilde{\psi}_i^s = \psi^s(x_i,t_{j+1}) \text{ on } \Gamma^{N,M}.
\end{aligned}$$

The nodal error is given by

$$v_{i,j+1} = \psi(x_i,t_{j+1}) - \widetilde{\psi}_i = (\psi^r(x_i,t_{j+1}) - \widetilde{\psi}_i^r) + (\psi^s(x_i,t_{j+1}) - \widetilde{\psi}_i^s).$$

To estimate the error in $\widetilde{\psi}_i$, we'll estimate the errors in $\widetilde{\psi}_i^r$ and $\widetilde{\psi}_i^s$ separately. From the differential equation and the result given in [123], we obtain

$$|\mathscr{L}^N(\psi^r(x_i,t_{j+1}) - \widetilde{\psi}_i^r)| \leq C\varepsilon(x_{i+1} - x_{i-1})|\psi^r(x_i,t_{j+1})|_3, \quad 0 \leq i \leq N.$$

The value of $|\psi^r(x_i,t_{j+1})|_3$ can be estimated by using Theorem 5.3.3 and the fact $x_{i+1} - x_{i-1} \leq 2N^{-1}$, to obtain

$$|\mathscr{L}^N(\psi^r(x_i,t_{j+1}) - \widetilde{\psi}_i^r)| \leq CN^{-1}, \quad 0 \leq i \leq N.$$

An application of Lemma 5.4.2 gives the following estimate

$$|\psi^r(x_i,t_{j+1}) - \widetilde{\psi}_i^r| \leq CN^{-1}, \quad 0 \leq i \leq N. \tag{5.4}$$

The error in the singular component is obtained by considering $\tau = 1/2$ and $\tau = \tau^*\sqrt{\varepsilon}\ln N$ separately. In the former case the mesh is uniform and $\tau^*\sqrt{\varepsilon}\ln N \geq \frac{1}{2}$. Then, using the classical argument, we obtain

$$|\mathscr{L}^N(\psi^s(x_i,t_{j+1}) - \widetilde{\psi}_i^s)| \leq C\varepsilon(x_{i+1} - x_{i-1})|\psi^s(x_i,t_{j+1})|_3.$$

Again the application of Theorem 5.3.3 and the fact $x_{i+1} - x_{i-1} = 2N^{-1}$, gives

$$|\mathscr{L}^N(\psi^s(x_i,t_{j+1}) - \widetilde{\psi}_i^s)| \leq CN^{-1}\varepsilon^{-1/2},$$

which gives

$$|\mathscr{L}^N(\psi^s(x_i,t_{j+1}) - \widetilde{\psi}_i^s)| \leq CN^{-1}\ln N.$$

A use of Lemma 5.4.2 yields

$$|\psi^s(x_i,t_{j+1}) - \widetilde{\psi}_i^s| \leq CN^{-1}\ln N. \tag{5.5}$$

In the latter case depending on the mesh spacing, a different argument is used to obtain an estimate on $|\psi^s(x_i,t_{j+1}) - \widetilde{\psi}_i^s|$. For $x_i$ in the subinterval $[0,\tau)$ the classical argument as used above gives

$$|\mathscr{L}^N(\psi^s(x_i,t_{j+1}) - \widetilde{\psi}_i^s)| \leq C\varepsilon(x_{i+1} - x_{i-1})|\psi^s(x_i,t_{j+1})|_3, \quad 0 \leq i \leq \frac{N}{2}.$$

Since the mesh width is $\frac{2\tau}{N}$ and $|\psi^s(x_i,t_{j+1})|_3 \leq C\varepsilon^{-3/2}$, therefore

$$|\mathscr{L}^N(\psi^s(x_i,t_{j+1}) - \widetilde{\psi}_i^s)| \leq CN^{-1}\frac{\tau}{\sqrt{\varepsilon}} \leq CN^{-1}\ln N, \quad 0 \leq i \leq \frac{N}{2}, \text{ as } \tau = \tau^*\sqrt{\varepsilon}\ln N. \tag{5.6}$$

On the other hand for $x_i \in [\tau, 1]$, we have

$$|\mathscr{L}^N(\psi^s(x_i,t_{j+1}) - \widetilde{\psi}_i^s)| = C\varepsilon\left(\delta^2 - \frac{d^2}{dx^2}\right)\psi^s(x_i,t_{j+1}), \quad \frac{N}{2} + 1 \leq i \leq N.$$

But $|\delta^2\psi^s(x_i,t_{j+1})| \leq \max_{x\in[x_{i-1},x_{i+1}]}|(\psi^s)''(x_i,t_{j+1})|$, and so

$$|\mathscr{L}^N(\psi^s(x_i,t_{j+1}) - \widetilde{\psi}_i^s)| \leq C\varepsilon \max_{x\in[x_{i-1},x_{i+1}]}|(\psi^s)''(x_i,t_{j+1})|, \quad \frac{N}{2} + 1 \leq i \leq N.$$

Using the estimates

$$|\mathscr{L}^N(\psi^s(x_i,t_{j+1}) - \widetilde{\psi}_i^s)| \leq C\begin{cases} e^{-\sqrt{\beta}(x_{i-1})/\sqrt{\varepsilon}}, & \text{if} \quad x_i \leq \frac{1}{2}, \\ e^{-\sqrt{\beta}(1-x_i)/\sqrt{\varepsilon}}, & \text{if} \quad x_i \geq \frac{1}{2}, \end{cases}$$

Now for $x_i \leq 1/2$, $x_i = \tau$ or $x_i > \tau$. If $x_i > \tau$ then $x_{i-1} \geq \tau$ and so

$$e^{-\sqrt{\beta}(x_{i-1})/\sqrt{\varepsilon}} \leq e^{-\sqrt{\beta}\tau/\sqrt{\varepsilon}} = N^{-1}.$$

Since $x_{i-1} = \tau - \frac{2\tau}{N}$ for $x_i = \tau$, so

$$\begin{aligned} e^{-\sqrt{\beta}(x_{i-1})/\sqrt{\varepsilon}} &= e^{-\sqrt{\beta}(\tau-\frac{2\tau}{N})/\sqrt{\varepsilon}} \\ &= e^{-\ln N}. \quad e^{2N^{-1}\ln N} \\ &= N^{-1}\left(N^{1/N}\right)^2 \leq CN^{-1}. \end{aligned}$$

It follows that

$$|\mathscr{L}^N(\psi^s(x_i,t_{j+1}) - \widetilde{\psi}_i^s)| \leq CN^{-1}, \quad \frac{N}{2}+1 \leq i \leq N. \tag{5.7}$$

The same result is obtained for the case of $x_i \geq 1/2$. Combining (5.6) and (5.7) gives

$$|\mathscr{L}^N(\psi^s(x_i,t_{j+1}) - \widetilde{\psi}_i^s)| \leq CN^{-1}\ln N, \quad 0 \leq i \leq N.$$

Thus the discrete minimum principle gives

$$|\psi^s(x_i,t_{j+1}) - \widetilde{\psi}_i^s| \leq CN^{-1}\ln N, \quad 0 \leq i \leq N. \tag{5.8}$$

The inequalities (5.4), (5.8) and the triangle inequality, give the required result. □

**Theorem 5.4.2** (Main Result)**.** *The solution $\widetilde{\psi}_i$ of the fully discretized scheme (5.3) converges uniformly to the solution $\psi(x,t)$ of (5.1) and the error estimate is given by*

$$|\psi(x_i,t_j) - \widetilde{\psi}_i| \leq C((\Delta t)^2 + N^{-1}\ln N), \quad i = 0,1,\ldots,N,\ j = 0,1,\ldots,M.$$

*Proof.* The proof immediately follows from Theorem 5.3.1 and Theorem 5.4.1. □

## 5.5 Numerical Illustrations

To verify the theoretical results computational results for two test problems are presented in the form of tables and graphs. To measure the accuracy of the method, for

each $\varepsilon$, the maximum absolute error is obtained as

$$e_{\varepsilon}^{N,M} = \max_{j}\left(\max_{i}|\widetilde{\psi}_{2i}^{2N,2M} - \widetilde{\psi}_{i}^{N,M}|\right),$$

where $\widetilde{\psi}_{i}^{N,M}$ and $\widetilde{\psi}_{2i}^{2N,2M}$ are the numerical solutions obtained at $j$-th level on $\mathscr{D}^{N,M}$ and $\mathscr{D}^{2N,2M}$ respectively. Note that the values of $\tau$ defined in Section 3 are different when we take $N$ and $2N$ partitions in the spatial direction which results in the mismatching at the nodal points. Thus the comparison of the solutions using the double mesh principle will not work. To fix this issue, the mesh $\mathscr{D}^{2N,2M}$ is obtained by the mesh $\mathscr{D}^{N,M}$ by inserting a new nodal point between two consecutive points (using the collocation method). The $\varepsilon$-uniform point-wise error given below is calculated over some range of $\varepsilon$

$$e^{N,M} = \max_{\varepsilon=1,2^{-4},2^{-8},\ldots,2^{-32}} e_{\varepsilon}^{N,M}.$$

Furthermore, the order of convergence $q_{\varepsilon}^{N,M}$ and the $\varepsilon$-uniform order of convergence $q^{N,M}$ are computed as

$$q_{\varepsilon}^{N,M} = \log_2\left(\frac{e_{\varepsilon}^{N,M}}{e_{\varepsilon}^{2N,2M}}\right), \text{ and } q^{N,M} = \log_2\left(\frac{e^{N,M}}{e^{2N,2M}}\right).$$

The following two test problems are encountered.

**Example 5.5.1.** First we consider

$$\begin{aligned}
&-\frac{\partial\psi(x,t)}{\partial t} + \varepsilon\frac{\partial^2\psi(x,t)}{\partial x^2} - x^p\frac{\partial\psi(x,t)}{\partial x} - \psi(x,t) = x^2 - 1,\ (x,t)\in\mathscr{D},\\
&\psi(x,0) = 0,\ 0\le x\le 1, \quad \psi(0,t) = t,\ \psi(1,t) = 0,\ 0\le t\le 1.
\end{aligned}$$

**Example 5.5.2.** Now we consider

$$\begin{aligned}
&-\frac{\partial\psi(x,t)}{\partial t} + \varepsilon\frac{\partial^2\psi(x,t)}{\partial x^2} - (2-x^2)x^p\frac{\partial\psi(x,t)}{\partial x} - (1+x)\psi(x,t)\\
&\qquad = 10t^2e^{-t}x(x-1),\ (x,t)\in\mathscr{D},\\
&\psi(x,0) = 1-x,\ 0\le x\le 1, \quad \psi(0,t) = 1+t^2,\ \psi(1,t) = 0,\ 0\le t\le 1.
\end{aligned}$$

**Table 5.1:** $e_{\varepsilon}^{N,M}$, $e^{N,M}$, $q_{\varepsilon}^{N,M}$ and $q^{N,M}$ for Example 5.5.1 for $p = 1$.

| $\varepsilon \downarrow N \rightarrow$ | 32 | 64 | 128 | 256 | 512 | 1024 |
|---|---|---|---|---|---|---|
| $2^{0}$ | 5.16e-04 | 2.69e-04 | 1.38e-04 | 6.95e-05 | 3.49e-05 | 1.75e-05 |
| | 0.94 | 0.96 | 0.99 | 0.99 | 0.99 | |
| $2^{-4}$ | 6.42e-03 | 2.56e-03 | 9.98e-04 | 4.09e-04 | 1.79e-04 | 6.20e-05 |
| | 1.33 | 1.36 | 1.29 | 1.19 | 1.53 | |
| $2^{-8}$ | 1.22e-02 | 5.68e-03 | 2.70e-03 | 1.31e-03 | 6.73e-04 | 3.41e-04 |
| | 1.10 | 1.07 | 1.04 | 0.96 | 0.98 | |
| $2^{-12}$ | 1.24e-02 | 5.98e-03 | 2.92e-03 | 1.58e-03 | 8.37e-04 | 4.36e-04 |
| | 1.05 | 1.03 | 0.89 | 0.92 | 0.94 | |
| $2^{-16}$ | 1.24e-02 | 5.99e-03 | 2.94e-03 | 1.60e-03 | 8.56e-04 | 4.49e-04 |
| | 1.05 | 1.03 | 0.88 | 0.90 | 0.93 | |
| $2^{-20}$ | 1.24e-02 | 5.99e-03 | 2.94e-03 | 1.60e-03 | 8.57e-04 | 4.50e-04 |
| | 1.05 | 1.03 | 0.88 | 0.90 | 0.93 | |
| $\vdots$ | $\vdots$ | $\vdots$ | $\vdots$ | $\vdots$ | $\vdots$ | |
| $2^{-32}$ | 1.24e-02 | 5.99e-03 | 2.94e-03 | 1.60e-03 | 8.57e-04 | 4.50e-04 |
| | 1.05 | 1.03 | 0.88 | 0.90 | 0.93 | |
| $e^{N,M}$ | 1.24e-02 | 5.99e-03 | 2.94e-03 | 1.60e-03 | 8.57e-04 | 4.50e-04 |
| $q^{N,M}$ | 1.05 | 1.03 | 0.88 | 0.90 | 0.93 | |

**Table 5.2:** $e_\varepsilon^{N,M}$ and $q_\varepsilon^{N,M}$ for Example 5.5.1 for $\varepsilon = 2^{-10}$ and different values of $p$.

| $p \downarrow N \rightarrow$ | 32 | 64 | 128 | 256 | 512 | 1024 |
|---|---|---|---|---|---|---|
| 2 | 1.11e-02 | 5.56e-03 | 3.07e-03 | 1.69e-03 | 8.96e-04 | 4.64e-04 |
| | 1.00 | 0.86 | 0.86 | 0.92 | 0.95 | |
| 4 | 1.11e-02 | 5.59e-03 | 3.26e-03 | 1.81e-03 | 9.60e-04 | 4.97e-04 |
| | 0.99 | 0.78 | 0.85 | 0.91 | 0.95 | |
| 6 | 1.11e-02 | 5.86e-03 | 3.30e-03 | 1.81e-03 | 9.53e-04 | 4.92e-04 |
| | 0.92 | 0.83 | 0.87 | 0.93 | 0.95 | |
| 8 | 1.11e-02 | 5.91e-03 | 3.29e-03 | 1.77e-03 | 9.29e-04 | 4.77e-04 |
| | 0.91 | 0.85 | 0.89 | 0.93 | 0.96 | |
| 10 | 1.13e-02 | 6.01e-03 | 3.23e-03 | 1.73e-03 | 9.00e-04 | 4.60e-04 |
| | 0.91 | 0.89 | 0.90 | 0.94 | 0.97 | |

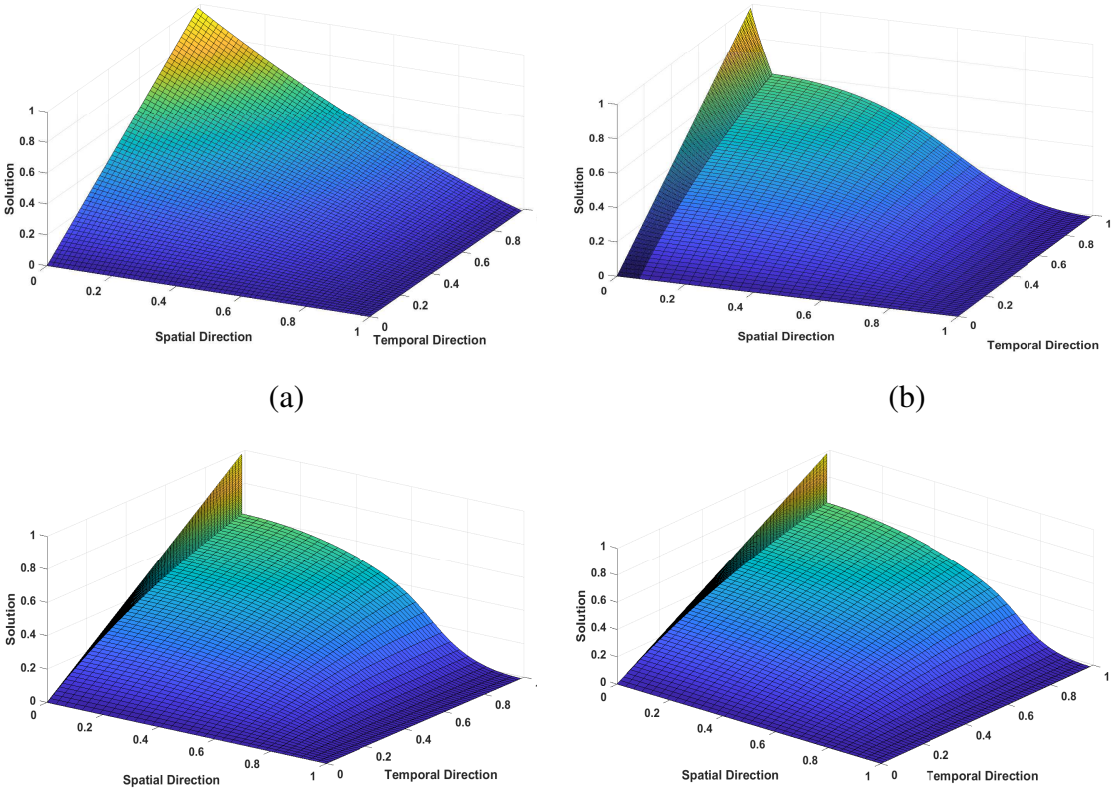


**Figure 5.1:** Numerical solution profiles for Example 5.5.1 for (a) $\varepsilon = 1, p = 1$ (b) $\varepsilon = 2^{-6}, p = 3$ (c) $\varepsilon = 2^{-12}, p = 5$ and (d) $\varepsilon = 2^{-18}, p = 7$.

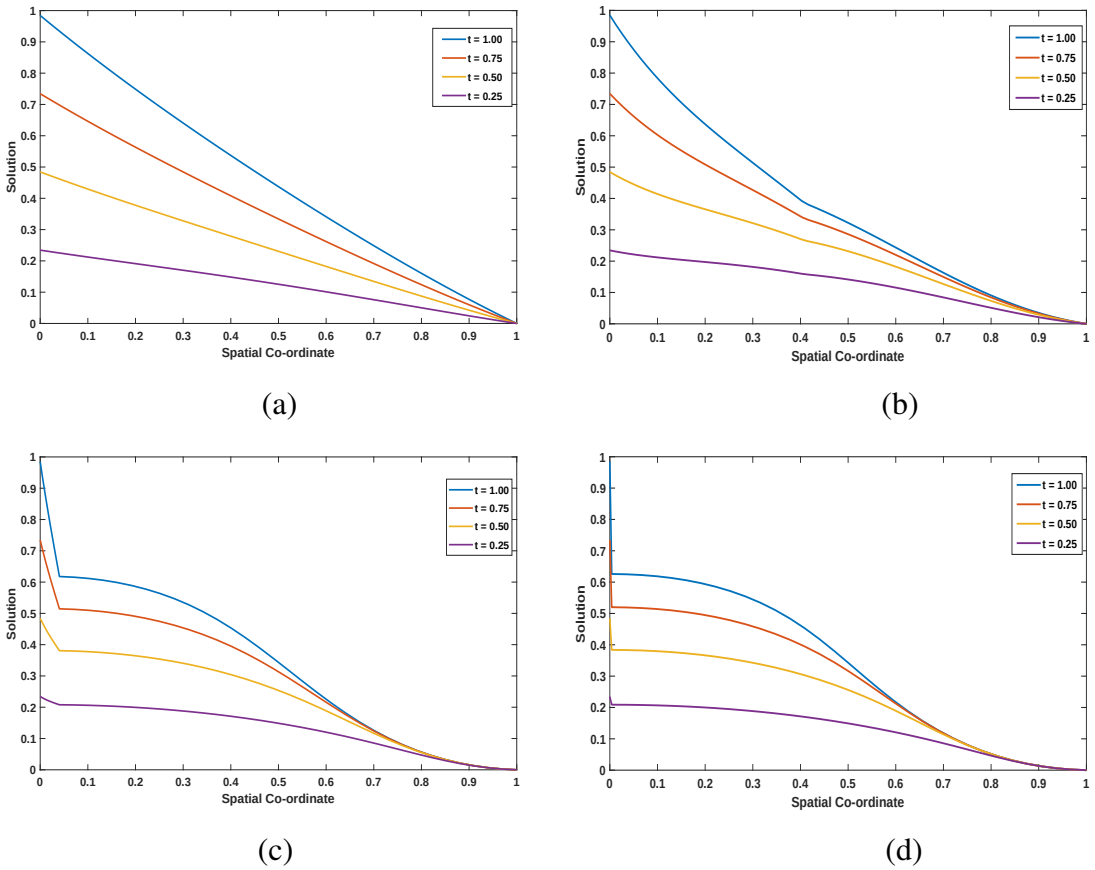


**Figure 5.2:** Numerical solution profiles for $p = 2$ at different time levels for Example 5.5.1 for (a) $\varepsilon = 1$ (b) $\varepsilon = 0.1$ (c) $\varepsilon = 0.01$ and (d) $\varepsilon = 0.001$.

**Table 5.3:** $e_{\varepsilon}^{N,M}$, $e^{N,M}$, $q_{\varepsilon}^{N,M}$ and $q^{N,M}$ for Example 5.5.2 for $p = 1$.

| $\varepsilon \downarrow N \rightarrow$ | 32 | 64 | 128 | 256 | 512 | 1024 |
|---|---|---|---|---|---|---|
| $2^{0}$ | 2.16e-03 | 1.03e-03 | 4.94e-04 | 2.44e-04 | 1.21e-04 | 6.00e-05 |
| | 1.07 | 1.06 | 1.02 | 1.01 | 1.01 | |
| $2^{-4}$ | 5.48e-03 | 3.54e-03 | 1.80e-03 | 9.06e-04 | 4.55e-04 | 2.28e-04 |
| | 0.63 | 0.97 | 0.99 | 0.99 | 1.00 | |
| $2^{-8}$ | 5.13e-02 | 2.43e-02 | 1.14e-02 | 5.19e-03 | 2.33e-03 | 1.02e-03 |
| | 1.08 | 1.09 | 1.13 | 1.15 | 1.19 | |
| $2^{-12}$ | 7.45e-02 | 3.76e-02 | 1.80e-02 | 8.82e-03 | 4.41e-03 | 2.21e-03 |
| | 0.99 | 1.06 | 1.03 | 1.00 | 1.00 | |
| $2^{-16}$ | 7.78e-02 | 4.16e-02 | 2.12e-02 | 1.02e-02 | 4.69e-03 | 2.26e-03 |
| | 0.90 | 0.97 | 1.05 | 1.12 | 1.05 | |
| $2^{-20}$ | 7.81e-02 | 4.20e-02 | 2.18e-02 | 1.11e-02 | 5.47e-03 | 2.58e-03 |
| | 0.89 | 0.95 | 0.97 | 1.02 | 1.08 | |
| $\vdots$ | $\vdots$ | $\vdots$ | $\vdots$ | $\vdots$ | $\vdots$ | |
| $2^{-32}$ | 7.81e-02 | 4.21e-02 | 2.19e-02 | 1.12e-02 | 5.63e-03 | 2.83e-03 |
| | 0.89 | 0.94 | 0.97 | 0.99 | 0.99 | |
| $e^{N,M}$ | 7.81e-02 | 4.21e-02 | 2.19e-02 | 1.12e-02 | 5.63e-03 | 2.83e-03 |
| $q^{N,M}$ | 0.89 | 0.94 | 0.97 | 0.99 | 0.99 | |

**Table 5.4:** $e_\varepsilon^{N,M}$ and $q_\varepsilon^{N,M}$ for Example 5.5.2 for $\varepsilon = 2^{-10}$ and different values of $p$.

| $p \downarrow N \rightarrow$ | 32 | 64 | 128 | 256 | 512 | 1024 |
|---|---|---|---|---|---|---|
| 2 | 5.44e-02 | 2.75e-02 | 1.42e-02 | 7.26e-03 | 3.64e-03 | 1.81e-03 |
| | 0.98 | 0.95 | 0.97 | 1.00 | 1.00 | |
| 4 | 5.34e-02 | 2.72e-02 | 1.42e-02 | 7.23e-03 | 3.63e-03 | 1.81e-03 |
| | 0.97 | 0.94 | 0.97 | 0.99 | 1.00 | |
| 6 | 5.34e-02 | 2.72e-02 | 1.42e-02 | 7.23e-03 | 3.63e-03 | 1.81e-03 |
| | 0.97 | 0.94 | 0.97 | 0.99 | 1.00 | |
| 8 | 5.34e-02 | 2.72e-02 | 1.42e-02 | 7.23e-03 | 3.63e-03 | 1.81e-03 |
| | 0.97 | 0.94 | 0.97 | 0.99 | 1.00 | |
| 10 | 5.34e-02 | 2.72e-02 | 1.42e-02 | 7.23e-03 | 3.63e-03 | 1.81e-03 |
| | 0.97 | 0.94 | 0.97 | 0.99 | 1.00 | |

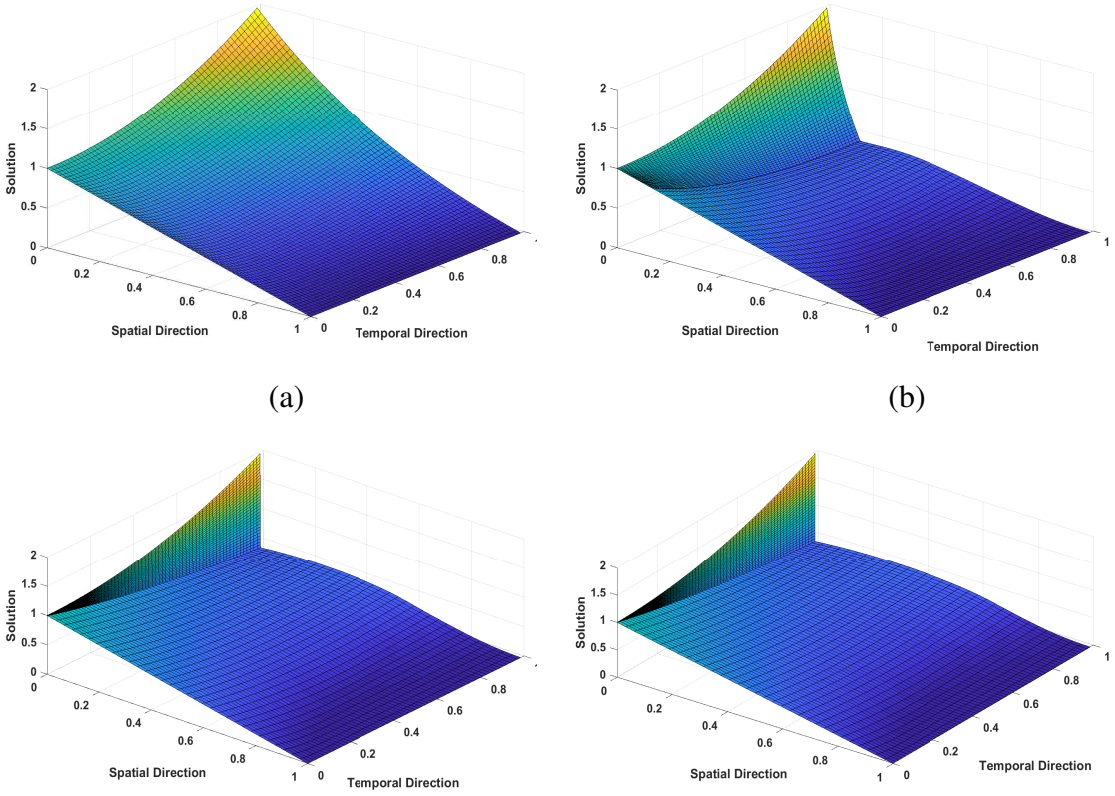


**Figure 5.3:** Numerical solution profiles for Example 5.5.2 for (a) $\varepsilon = 1, p = 1$ (b) $\varepsilon = 2^{-6}, p = 3$ (c) $\varepsilon = 2^{-12}, p = 5$ and (d) $\varepsilon = 2^{-18}, p = 7$.

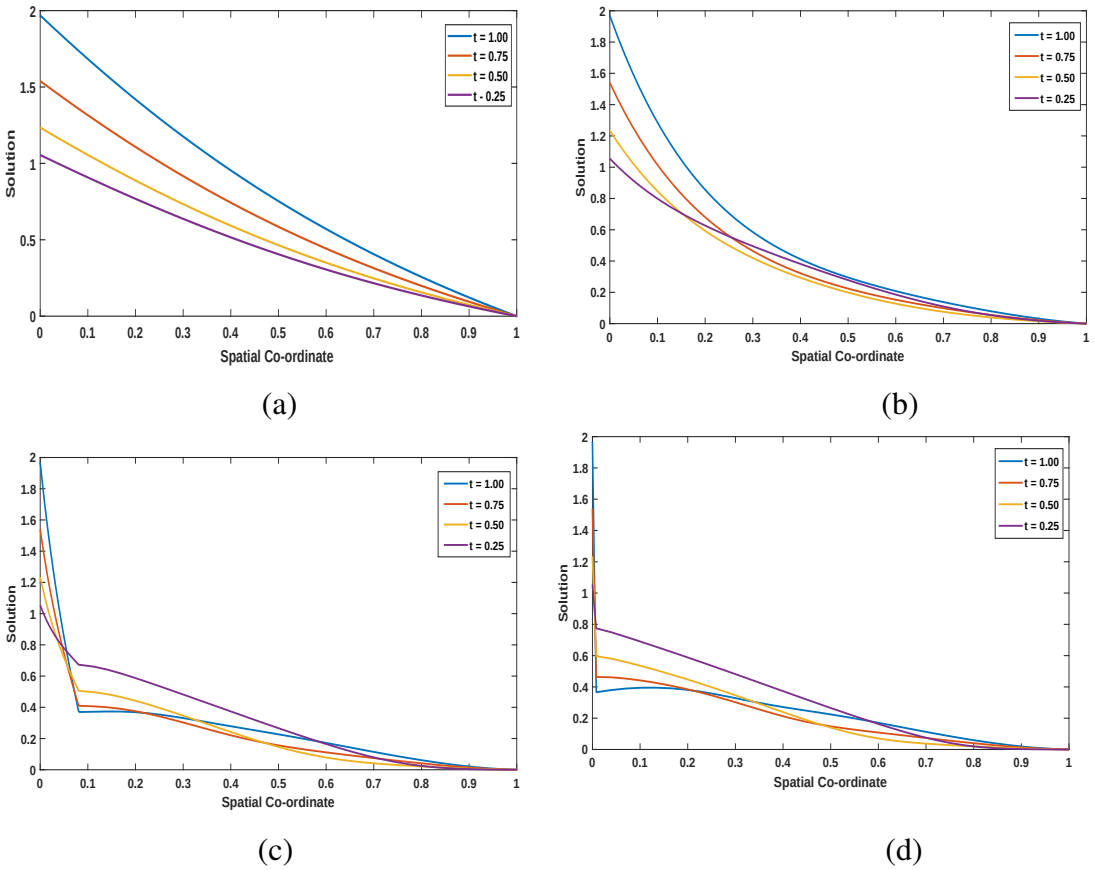


**Figure 5.4:** Numerical solution profiles for $p = 2$ at different time levels for Example 5.5.2 for (a) $\varepsilon = 1$ (b) $\varepsilon = 0.1$ (c) $\varepsilon = 0.01$ and (d) $\varepsilon = 0.001$.

The numerical results presented in the tables confirm the theoretical results proved in Theorem 5.4.2 which clearly show the $\varepsilon$-uniform convergence of the method. All the results presented in Tables 5.1-5.4 are obtained by taking $M = N$. Also, we have used 64 points in both directions to plot all the graphs. To observe the change in the boundary layer width with respect to the parameter and to show the physical phenomenon of the solution, the surface plots (refer Fig. 5.1 and Fig. 5.3) have been presented. From these figures, one can observe that the solution exhibits a boundary layer at $x = 0$ for small $\varepsilon$, and the boundary layer width decreases as the parameter decreases. To see the solution at some individual time steps, the solution behavior for different time levels is also drawn (refer Figs. 5.2 and Figs. 5.4).

## 5.6 Conclusion

We proposed parameter-uniform numerical scheme of $\mathscr{O}((\Delta t)^2 + N^{-1}\ln N)$ for SPB-VPs with a boundary turning point. The presence of $\varepsilon$ and the boundary turning point make these problems more difficult to solve numerically. The uniform-convergence is proved through a rigorous analysis. The method can also be extended to the reaction-diffusion SPBVPs whose solution exhibits parabolic boundary layers on both sides of the domain as $\varepsilon$ approaches zero. The analysis is also valid for $p = 0$ when the solution, in general, has a different kind of layer than the layer that appears in our problem. Two test examples are encountered to check the accuracy and efficiency of the method.